

# Effects of Inductance on the Propagation Delay and Repeater Insertion in VLSI Circuits

Yehea I. Ismail and Eby G. Friedman, *Fellow, IEEE*

**Abstract**—A closed-form expression for the propagation delay of a CMOS gate driving a distributed *RLC* line is introduced that is within 5% of dynamic circuit simulations for a wide range of *RLC* loads. It is shown that the error in the propagation delay if inductance is neglected and the interconnect is treated as a distributed *RC* line can be over 35% for current on-chip interconnect. It is also shown that the traditional quadratic dependence of the propagation delay on the length of the interconnect for *RC* lines approaches a linear dependence as inductance effects increase. On-chip inductance is therefore expected to have a profound effect on traditional high-performance integrated circuit (IC) design methodologies.

The closed-form delay model is applied to the problem of repeater insertion in *RLC* interconnect. Closed-form solutions are presented for inserting repeaters into *RLC* lines that are highly accurate with respect to numerical solutions. *RC* models can create errors of up to 30% in the total propagation delay of a repeater system as compared to the optimal delay if inductance is considered. The error between the *RC* and *RLC* models increases as the gate parasitic impedances decrease with technology scaling. Thus, the importance of inductance in high-performance very large scale integration (VLSI) design methodologies will increase as technologies scale.

**Index Terms**—CMOS, high-performance, high-speed interconnect, propagation delay, VLSI.

## I. INTRODUCTION

IT HAS become well accepted that interconnect delay dominates gate delay in current deep submicrometer very large scale integration (VLSI) circuits [1]–[8]. With the continuous scaling of technology and increased die area, this behavior is expected to continue. In order to properly design complex circuits, more accurate interconnect models and signal propagation characterization are required. Historically, interconnect has been modeled as a single lumped capacitance in the analysis of the performance of on-chip interconnects. With the scaling of technology and increased chip sizes, the cross-sectional area of wires has been scaled down while interconnect length has increased. The resistance of the interconnect has therefore increased in significance, requiring the use of more accurate *RC* delay models [5].

Manuscript received January 26, 1999; revised May 13, 1999 and August 23, 1999. This work was supported in part by the National Science Foundation under Grant MIP-9610108, the Semiconductor Research Corporation under Contract 99-TJ-687, a grant from the New York State Science and Technology Foundation to the Center for Advanced Technology-Electronic Imaging Systems, and by grants from the Xerox Corporation, IBM Corporation, Intel Corporation, and Lucent Technologies Corporation.

The authors are with the Department of Electrical and Computer Engineering, University of Rochester, Rochester, NY 14627 USA.

Publisher Item Identifier S 1063-8210(00)01027-1.

Currently, inductance is becoming more important with faster on-chip rise times and longer wire lengths. Wide wires are frequently encountered in clock distribution networks and in upper metal layers. These wires are low-resistance wires that can exhibit significant inductive effects. Furthermore, increasing performance requirements are pushing the introduction of new materials for low-resistance interconnect [9]. With these trends, it is becoming more important to include inductance when modeling on-chip interconnect. Criteria to determine which nets should consider on-chip inductance have been described in [10]–[13].

The focus of this paper is to provide an accurate estimation of the propagation delay of a CMOS gate driving a distributed *RLC* line as well as to develop design expressions for optimum repeater insertion to minimize the delay of a signal propagating along a distributed *RLC* line. Repeaters are often used to minimize the delay required to propagate a signal through those interconnect lines that are best modeled as an *RC* impedance [14]–[19]. Thus, the objective of this paper is to highlight the significance of increasing inductance effects in current VLSI circuits with respect to on-chip interconnect and repeater insertion in *RLC* lines.

The paper is organized as follows. In Section II, a simple yet accurate propagation delay formula describing a gate driving a distributed *RLC* load is presented. In Section III, the propagation delay formula is used to develop design expressions for optimum repeater insertion to minimize the propagation delay of a distributed *RLC* line. Some conclusions are offered in Section IV. Practical industrial numbers are used to characterize the importance of inductance in current VLSI circuits in Appendix A. A mathematical proof of the expressions for optimum repeater insertion in an *RLC* line is provided in Appendix B.

## II. PROPAGATION DELAY OF A CMOS GATE DRIVING AN *RLC* LOAD

A simple yet accurate formula characterizing the propagation delay of a CMOS gate driving an *RLC* transmission line is presented in Section II-A. The closed-form solution for the propagation delay is shown to be within 5% error of AS/X<sup>1</sup> [20] simulations for a wide range of *RLC* lines. In Section II-B, the closed-form solution for the propagation delay is shown to accurately describe the special case of an *RC* line as  $L \rightarrow 0$ . The solution for the propagation delay including inductance is compared to the case where inductance is neglected and the line is treated as an *RC* line, permitting the error due to neglecting inductance to be quantified. In Section II-C, the dependence of the

<sup>1</sup>AS/X is a dynamic circuit simulator developed and used by IBM. AS/X is similar to SPICE, but has a specific emphasis on transmission line networks and uses the ASTAP language for describing the circuit in the input files.

propagation delay on the length of an interconnect line is investigated. It is shown that the traditional quadratic dependence of the propagation delay on the length of the interconnect for an  $RC$  line tends to a linear relation as inductance effects increase.

### A. Propagation Delay Formula

A gate driving an  $RLC$  transmission line representation of an interconnect line is shown in Fig. 1.  $R_t$ ,  $L_t$ , and  $C_t$  are the total resistance, inductance, and capacitance of the line, respectively. The line parameters  $R_t$ ,  $L_t$ , and  $C_t$  are given by  $R_t = Rl$ ,  $L_t = Ll$ , and  $C_t = Cl$ , respectively, where  $R$ ,  $L$ , and  $C$  are the resistance, inductance, and capacitance per unit length of the interconnect and  $l$  is the length of the line. The conductance of the line  $G$  is neglected since at current operating frequencies the capacitive impedance dominates the parallel semiconductor conductance.  $R_{tr}$  is the equivalent output resistance of the gate driving the interconnect.  $C_L$  is the input capacitance of the following gate at the end of the interconnect section. A minimum size buffer has an output resistance  $R_0$  and an input capacitance  $C_0$ . The input voltage  $V_{in}$  is a fast rising signal that can be approximated by a step signal.  $V_{out}$  is the far output voltage at the end of the interconnect section.

From the basic principles of a transmission lines [21], the transfer function of a lossy transmission line with a source impedance  $z_s$  and a load impedance  $z_L$ ,  $V_{out}(s)/V_{in}(s)$  is given by

$$\frac{V_{out}(s)}{V_{in}(s)} = \frac{2}{\left(\frac{z_s}{z_0} + 1\right) \left(\frac{z_0}{z_L} + 1\right) e^{\gamma l} + \left(\frac{z_s}{z_0} - 1\right) \left(\frac{z_0}{z_L} - 1\right) e^{-\gamma l}} \quad (1)$$

where  $\gamma$  and  $z_0$  are the propagation constant and the characteristic impedance of the line and are given by

$$z_0 = \sqrt{\frac{L_t}{C_t}} \sqrt{1 + \frac{R_t}{sL_t}} \quad (2)$$

$$\gamma l = s\sqrt{L_t C_t} \sqrt{1 + \frac{R_t}{sL_t}}. \quad (3)$$

For a CMOS gate driving another CMOS gate at the end of the line,  $z_s = R_{tr}$  and  $z_L = 1/sC_L$ . A time scaling is applied by substituting  $t'/\omega_n$  for each  $t$  where

$$\omega_n = \frac{1}{\sqrt{L_t(C_t + C_L)}}. \quad (4)$$

From the characteristics of the Laplace transform, the complex frequency  $s$  is substituted by  $\omega_n s'$ . With this time scaling, the variables  $\gamma$ ,  $z_0$ , and  $z_L$  are transformed to  $\gamma'$ ,  $z'_0$ , and  $z'_L$ , respectively, which can be evaluated by substituting  $\omega_n s'$  for each  $s$  and are

$$\gamma' l = \frac{s'}{\sqrt{1 + C_T}} \sqrt{1 + \frac{2\zeta_{line}}{s'} \sqrt{1 + C_T}} \quad (5)$$

$$z'_0 = \sqrt{\frac{L_t}{C_t}} \sqrt{1 + \frac{2\zeta_{line}}{s'} \sqrt{1 + C_T}} \quad (6)$$

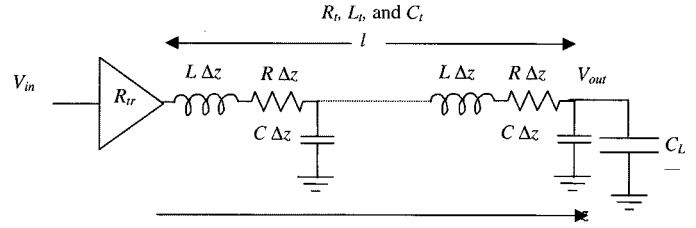


Fig. 1. A gate driving an  $RLC$  transmission line.

$$z'_L = \sqrt{\frac{L_t}{C_t}} \frac{1}{s'} \frac{\sqrt{1 + C_T}}{C_T} \quad (7)$$

where

$$C_T = \frac{C_L}{C_t} \quad (8)$$

$$\zeta_{line} = \frac{R_t}{2} \sqrt{\frac{C_t}{L_t}}. \quad (9)$$

Using the above expressions, the impedance ratios describing the transfer function in (1) become

$$\frac{z'_0}{z'_L} = \frac{1}{s'} \sqrt{1 + \frac{2\zeta_{line}}{s'} \sqrt{1 + C_T}} \frac{\sqrt{1 + C_T}}{C_T} \quad (10)$$

$$\frac{z'_s}{z'_0} = \frac{2R_{tr}\zeta_{line}}{\sqrt{1 + \frac{2\zeta_{line}}{s'} \sqrt{1 + C_T}}} \quad (11)$$

where

$$R_T = \frac{R_{tr}}{R_t}. \quad (12)$$

Referring to the transfer function in (1), (5), (10), and (11), the scaled transfer function in terms of  $s'$  is a function of only three variables:  $\zeta_{line}$ ,  $R_T$ , and  $C_T$ . The canonical number of variables to characterize the scaled transfer function in terms of  $s'$  is three. There are numerous ways to select the three variables that characterize the scaled transfer function. Three variables are chosen to simplify the process for determining the 50% delay point, which is the target of this analysis. Thus, the three variables,  $\zeta$ ,  $R_T$ , and  $C_T$ , are chosen to describe the transformed transfer function, where

$$\zeta = \frac{R_t}{2} \sqrt{\frac{C_t}{L_t}} \cdot \frac{R_T + C_T + R_T C_T + 0.5}{\sqrt{(1 + C_T)}} = \zeta_{line} \frac{R_T + C_T + R_T C_T + 0.5}{\sqrt{(1 + C_T)}}. \quad (13)$$

The variables,  $R_T$  and  $C_T$ , characterize the relative significance of the gate parasitic impedances with respect to the parasitic interconnect impedances. Increasing  $R_T$  and  $C_T$  demonstrates that the gate parasitic impedances further affect the propagation delay. To clarify the process for selecting the third variable  $\zeta$ , the transfer function is expressed as a series in the powers of  $s'$ . The exponential functions in the transfer function in (1) are replaced by a series expansion, resulting in (14), given at the bottom of the next page. The first few terms of the series expansion in powers of  $s'$  are given in (15), also at the bottom of the next page. The third variable  $\zeta$  is the coefficient of  $s^1$  in the denominator of the transfer function.  $\zeta$  is chosen as the third

variable since the 50% delay is primarily dependent on the coefficients of  $s^1$  in the denominator and the numerator [22]. This characteristic is used to reduce the number of variables that affect the propagation delay from three to one ( $\zeta$ ). Note that the three variables,  $R_T$ ,  $C_T$ , and  $\zeta$ , are not independent since  $\zeta$  is a function of  $R_T$  and  $C_T$ . Note also that (14) and (15) show the first terms of the series expansion of the transfer function in powers of  $s'$  and do not represent any truncation in the transfer function. The coefficients of powers of  $s'$  are functions of only the three variables,  $R_T$ ,  $C_T$ , and  $\zeta$ , for any power as described by (1), (5), (10), and (11).

For a unit step input function, the output voltage waveform  $V_{\text{out}}(t') = \mathcal{L}^{-1}\{(1/s)*V_{\text{out}}(s')/V_{\text{in}}(s')\}$  is also a function of the three variables,  $\zeta$ ,  $R_T$ , and  $C_T$ . The scaled 50% propagation delay  $t'_{pd}$  can be calculated by solving  $V_{\text{out}}(t'_{pd}, \zeta, R_T, C_T) = 0.5$  which means that  $t'_{pd}$  is only a function of  $\zeta$ ,  $R_T$ , and  $C_T$ . Thus, the propagation delay of an  $RLC$  line with a source resistance  $R_{tr}$  and a load capacitance  $C_L$  has the form

$$t_{pd} = \frac{t'_{pd}(\zeta, R_T, C_T)}{\omega_n}. \quad (16)$$

The scaled propagation delay  $t'_{pd}$  is dimensionless since  $\omega_n$  has the units of 1/time. Note that this solution is a characteristic of an  $RLC$  line and that no approximations have been made in deriving this result.

As described in (16), the same value of the scaled 50% delay  $t'_{pd}$  results in many different transmission line configurations driven by a step input supply with a source resistance and a load capacitance. The value of  $t'_{pd}$  remains constant as long as  $R_t$ ,  $L_t$ ,  $C_t$ ,  $R_{tr}$ , and  $C_L$  scale such that  $\zeta$ ,  $R_T$ , and  $C_T$  are constant. Thus, simulations are used to characterize  $t'_{pd}$  as a function of  $\zeta$ ,  $R_T$ , and  $C_T$  based on the parameters,  $R_t$ ,  $L_t$ ,  $C_t$ ,  $R_{tr}$ , and  $C_L$ . The resulting expression for  $t'_{pd}$  is guaranteed to correctly characterize any combination of the parameters  $R_t$ ,  $L_t$ ,  $C_t$ ,  $R_{tr}$ , and  $C_L$ . AS/X [20] simulations of the time-scaled 50% propagation delay  $t'_{pd}$  of a gate driving an  $RLC$  transmission line as a function of  $\zeta$ ,  $R_T$ , and  $C_T$  are shown in Fig. 2. The simulations depicted in Fig. 2 for the curve with  $R_T = 0$  and  $C_T = 0$  are performed with  $R_t = 50 \Omega$ ,  $C_t = 1 \text{ pF}$ ,  $R_{tr} = 0$ , and  $C_L = 0$ , and  $L_t$  is varied to vary  $\zeta$ . AS/X is used to determine the 50% delay  $t_{pd}$  for each value of  $L_t$ . The result is multiplied by  $\omega_n$  in (4) to determine  $t'_{pd}$ .

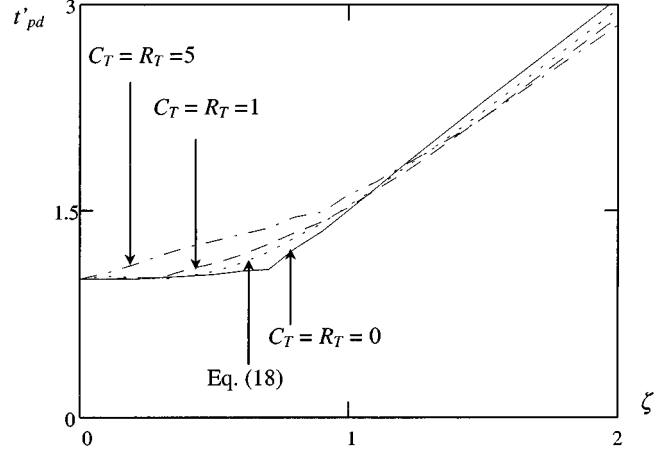


Fig. 2. Comparison of the accuracy of (18) to AS/X [20] simulations of the time-scaled 50% propagation delay  $t'_{pd}$  of an  $RLC$  transmission line with a source resistance  $R_{tr}$  and a load capacitance  $C_L$ . The propagation delay is plotted versus  $\zeta$  for different values of  $R_T$  and  $C_T$ .

For the curve with  $R_T = 1$  and  $C_T = 1$ , the same procedure is used, but with  $R_{tr} = 50 \Omega$  and  $C_L = 1 \text{ pF}$ . For the curve with  $R_T = 5$  and  $C_T = 5$ ,  $R_{tr} = 250 \Omega$  and  $C_L = 5 \text{ pF}$ . The specific values of the parameters ( $R_t$ ,  $L_t$ ,  $C_t$ ,  $R_{tr}$ , and  $C_L$ ) used in the simulations shown in Fig. 2 are not important as long as the required ranges of  $\zeta$ ,  $R_T$ , and  $C_T$  are satisfied. For the cases where the output response crosses the 50% point several times due to severe ringing, the propagation delay is calculated based on the final crossing which represents the worst case delay. Note in Fig. 2 that the propagation delay is primarily a function of  $\zeta$ . The dependence on  $R_T$  and  $C_T$  is fairly weak. This characteristic does not imply that the transistor driving the interconnect and the load capacitance has a weak effect on the propagation delay since  $\zeta$  includes the effects of  $R_T$  and  $C_T$  as given by (13). Only the extra effect of  $R_T$  and  $C_T$  that is not included in  $\zeta$  is neglected. Note also that this effect is particularly weak in the range where  $R_T$  and  $C_T$  are between zero and one. This range is most important for global interconnect and long wires in current deep submicrometer technologies. Thus, the propagation delay is primarily a function of  $\zeta$ , which collects the five parameters that affect the propagation delay,  $R_t$ ,  $L_t$ ,  $C_t$ ,  $R_{tr}$ , and  $C_L$ , into a single parameter. The time-scaled propagation delay  $t'_{pd}$  is considered as a function of only  $\zeta$  in the range where  $R_T$

$$\frac{V_{\text{out}}(s')}{V_{\text{in}}(s')} = \frac{1}{\left(1 + \frac{z_s}{z'_L}\right) \left(1 + \frac{(\gamma'l)^2}{2!} + \dots\right) + \left(\frac{z_s}{z'_0} + \frac{z'_0}{z'_L}\right) \left((\gamma'l) + \frac{(\gamma'l)^3}{3!} + \dots\right)} \quad (14)$$

$$\frac{V_{\text{out}}(s')}{V_{\text{in}}(s')} = \frac{1}{1 + 2\zeta s' + \left(\frac{0.5 + C_T}{1 + C_T} + 16\zeta^2 \left(1 - \frac{R_T^2 + C_T^2 + (R_T C_T)^2}{(R_T + C_T + R_T C_T + 0.5)^2}\right)\right) s'^2 + \dots} \quad (15)$$

TABLE I  
COMPARISON OF  $t_{pd}$  IN (18) TO AS/X SIMULATIONS CHARACTERIZING THE PROPAGATION DELAY OF A GATE DRIVING AN  $RLC$  TRANSMISSION LINE.  $C_t = 1$  pF  
AND  $R_{tr} = 25 \Omega$ . THE SHADED ROWS REPRESENT THE SIMULATED CASES SHOWN IN FIG. 3

$R_T$	$L_t$ (nH)	$C_T = 0.1$				$C_T = 0.5$				$C_T = 1.0$			
		$\zeta$ (13)	(18) (ps)	AS/X (ps)	Error	$\zeta$ (13)	(18) (ps)	AS/X (ps)	Error	$\zeta$ (13)	(18) (ps)	AS/X (ps)	Error
0.1	2	1.89	131	134	2.2%	2.62	213	214	0.5%	3.36	314	311	1.0%
	5	1.19	133	135	1.5%	1.66	213	216	1.4%	2.12	314	313	0.3%
	8	0.94	138	137	0.7%	1.31	214	218	1.8%	1.68	315	316	0.3%
	10	0.84	142	138	2.9%	1.17	216	219	1.4%	1.503	315	320	1.6%
0.5	2	0.61	53	51	3.9%	0.80	71	71	0.0%	0.99	96	98	2.0%
	5	0.34	76	77	1.3%	0.50	92	95	3.1%	0.62	114	117	2.5%
	8	0.31	95	96	1.0%	0.40	112	115	2.6%	0.49	134	140	4.2%
	10	0.27	106	107	0.9%	0.36	124	126	1.6%	0.44	146	152	3.9%
1.0	2	0.45	49	49	0.0%	0.57	60	61	1.6%	0.69	75	78	3.8%
	5	0.29	75	76	1.3%	0.36	88	88	0.0%	0.44	103	108	4.6%
	8	0.23	95	95	0.0%	0.28	110	110	0.0%	0.34	128	131	2.3%
	10	0.20	106	106	0.0%	0.25	124	121	2.4%	0.31	143	144	0.7%

and  $C_T$  are between zero and one and the propagation delay is given by

$$t_{pd} \approx \frac{t'_{pd}(\zeta)}{\omega_n}. \quad (17)$$

Approximating the time-scaled propagation delay  $t'_{pd}$  as a function of only one variable allows simple one-dimensional (1-D) curve-fitting methods to be applied to determine an expression describing the 50% delay. A curve-fitting method is used to minimize the error when  $R_T$  and  $C_T$  are between zero and one as shown in Fig. 2, resulting in the following expression for the 50% propagation delay:

$$t_{pd} = (e^{-2.9\zeta^{1.35}} + 1.48\zeta)/\omega_n. \quad (18)$$

AS/X [20] simulations of the propagation delay of an  $RLC$  transmission line as compared to  $t_{pd}$  in (18) are shown in Table I. Note that the solution exhibits high accuracy (the maximum error is 4.6% and the average error is 1.65%) for a wide range of interconnect ( $R_t$ ,  $L_t$ , and  $C_t$ ) and gate impedances ( $R_{tr}$  and  $C_L$ ). Values of  $\zeta$  are calculated and listed in Table I for the simulated cases, which varies from 3.36 to 0.20. Thus, the simulation data listed in Table I include those cases with high inductive effects where the response is underdamped and overshoots occur (small  $\zeta$ ) and those cases with low-inductive effects where the response is overdamped (large  $\zeta$ ). Equation (18) characterizes the propagation delay accurately for any set of parameters,  $R_t$ ,  $L_t$ ,  $C_t$ ,  $R_{tr}$ , and  $C_L$ , for which  $R_T$  and  $C_T$  are in the range between zero and one and any value of  $\zeta$ . Actually, (18) suffers high errors only in the region where  $C_T$  and  $R_T$  are high and  $\zeta$  is low. This case can only occur for unreasonably high values of the inductance per unit length of the line as compared to the resistance and capacitance per unit length of the line. Such a case does not exist in a practical VLSI circuit. So the delay model is therefore accurate for any practical line and gate. Alternatively, as the load capacitance and gate resistance increase (increasing  $R_T$  and  $C_T$ ),  $\zeta$  increases. Note in Fig. 2 that the error for high  $\zeta$  is low (below 5%).

The parameter  $\zeta$  can be used to characterize inductance effects more accurately and comprehensively than the figures of merit developed in [10]–[13]. To better explain this point, note that  $\zeta$  can be rewritten as

$$\zeta = \frac{1}{2\sqrt{(1+C_T)}} \left[ \frac{R_t}{2Z_{0l}} + \frac{R_{tr}}{Z_{0l}} + \frac{\tau_{CL}}{\tau_f} \right] \quad (19)$$

where  $Z_{0l} = \sqrt{L_t/C_t}$  is the characteristic impedance of a lossless transmission line,  $\tau_{CL} = C_L(R_t + R_{tr})$  is the time constant for charging the load capacitance  $C_L$  through the gate and wire resistances, and  $\tau_f = \sqrt{L_t C_t}$  is the time of flight of the signals propagating across the transmission line. Thus, (19) characterizes three different factors that determine inductance effects in  $RLC$  lines. The first factor is the total line resistance  $R_t$  as compared to the lossless characteristic impedance of the line  $Z_{0l}$ . If the ratio of the total resistance of the line to the lossless characteristic impedance increases, inductance effects can be neglected. The second factor is the ratio between the driver resistance  $R_{tr}$  and the lossless characteristic impedance of the line. If this ratio increases, inductance effects can be neglected. The last factor is the ratio between the time required to charge  $C_L$  through the gate and wire resistances to the time of flight of the signals propagating across the line. If this ratio increases, inductance effects can be neglected. The three factors are collected in the single metric  $\zeta$  which is sufficient to characterize inductance effects exhibited by an  $RLC$  line and includes the effects of the driver output resistance and the load capacitance. The same three factors are characterized in [12] by three separate inequalities that have to be simultaneously satisfied for inductance effects to be important.<sup>2</sup> The difficulty with this approach is that certain cases exist where each of these factors separately tested for inductance effects would predict that the line would suffer inductance effects while actually the line would suffer no inductance effects due to the *combined* effect of the three factors. The single metric  $\zeta$  introduced here accurately models the combined effect of these three factors, which is represented by

<sup>2</sup>The load capacitor metric in [12] is different from the metric introduced here.

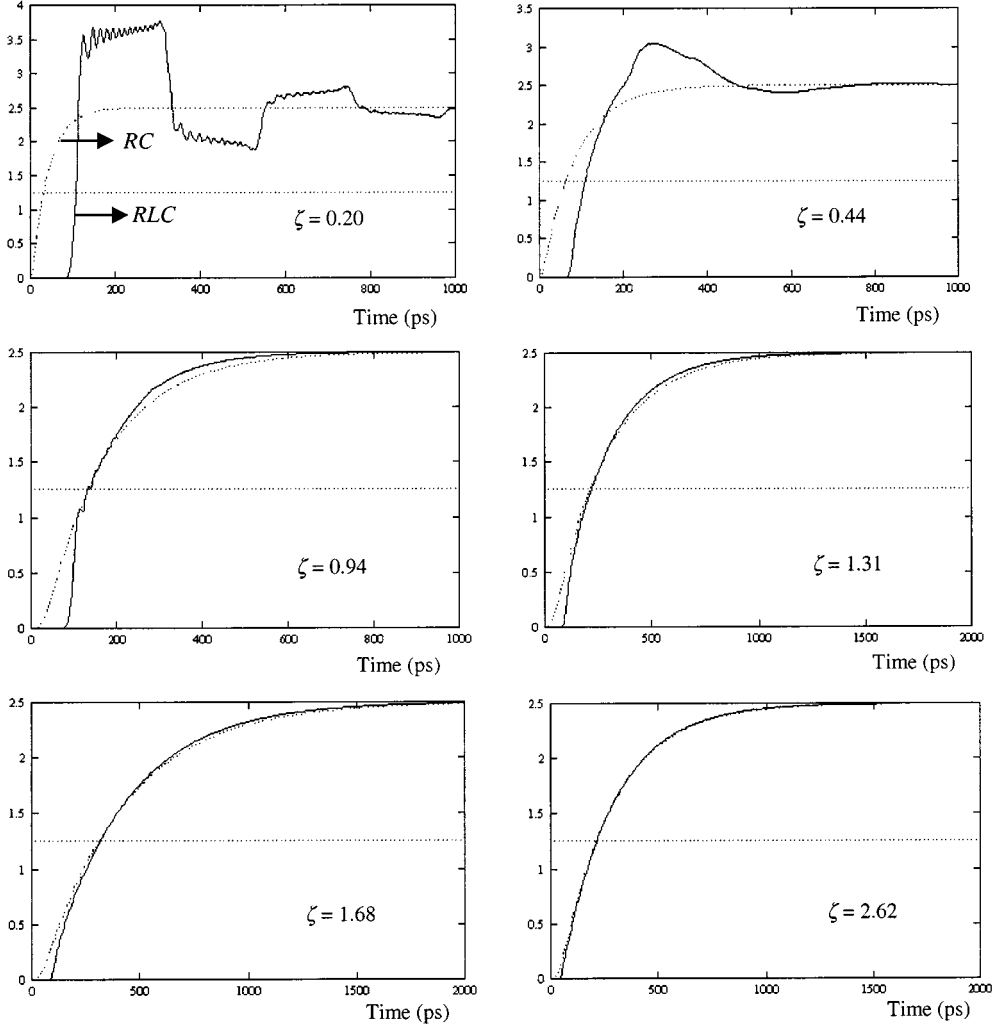


Fig. 3. Circuit simulations comparing an  $RLC$  interconnect model to an  $RC$  interconnect model for the shaded cells in Table I. The metric  $\zeta$  in (13) is shown within each individual graph.

the addition in (19). Simulations comparing an  $RLC$  to an  $RC$  interconnect model for the shaded cells in Table I are depicted in Fig. 3. Note that the error due to neglecting inductance is insignificant for  $\zeta > 1.5$ . Note also that the effect of the rise time of the input signal on the significance of inductance is not considered here, but is characterized in [13].

### B. Comparison to an $RC$ Model

The propagation delay  $t_{pd}$  in (18) can be rewritten as

$$t_{pd} = \frac{e^{-2.9\zeta^{1.35}}}{\omega_n} + 0.74R_tC_t(R_T + C_T + R_TC_T + 0.5). \quad (20)$$

To examine how accurately the closed-form solution of the propagation delay of an  $RLC$  transmission line in (20) characterizes the special case of a distributed  $RC$  line, (20) is evaluated when inductance becomes negligible. As given by (4) and (13),  $\omega_n \rightarrow \infty$  and  $\zeta \rightarrow \infty$  as  $L_t \rightarrow 0$  and thus

$$t_{pd}(RC) = 0.74R_tC_t(R_T + C_T + R_TC_T + 0.5) \quad (21)$$

which can be rearranged into

$$t_{pd}(RC) = 0.37R_tC_t + 0.74(R_tC_L + R_{tr}C_t + R_{tr}C_L). \quad (22)$$

Note the similarity of this expression to the expressions for the propagation delay of a distributed  $RC$  line in [5] and [16]. Thus, the general expression for the propagation delay of a CMOS gate driving an  $RLC$  interconnect described by (18) also includes the special case of an  $RC$  interconnect. Note also that the term  $1.48\zeta/\omega_n$  in (18) is  $t_{pd}(RC)$ . Thus, (18) can be viewed as the traditional  $RC$  delay plus a correction term representing the effects of inductance.

The error encountered when neglecting the inductance of an interconnect line and treating the line as an  $RC$  line is quantified by the expression  $(t_{pd}(RLC) - t_{pd}(RC))/t_{pd}(RLC)$ .  $t_{pd}(RLC)$  is given by (18) and  $t_{pd}(RC)$  is given by  $1.48\zeta/\omega_n$ . The percent error with these expressions is

$$\%Error = \frac{100e^{-2.9\zeta^{1.35}}}{e^{-2.9\zeta^{1.35}} + 1.48\zeta}. \quad (23)$$

Note that the error is only a function of  $\zeta$ . Equation (23) and AS/X simulations are plotted in Fig. 4. The closed-form solu-

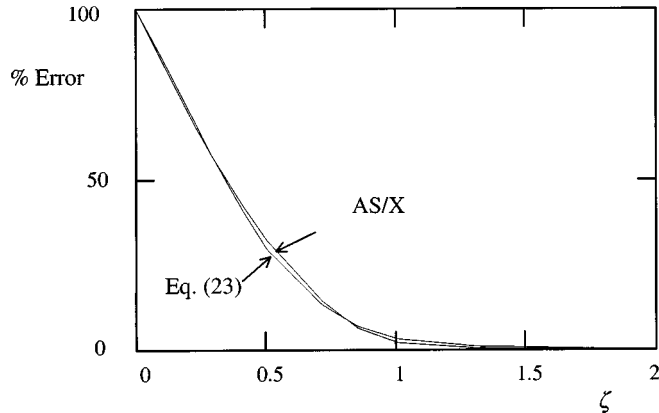


Fig. 4. Equation (23) as compared to AS/X simulations describing the error between an  $RLC$  transmission line model and an  $RC$  transmission line model.  $R_t = 30 \Omega$ ,  $C_t = 1$  pF,  $R_T = C_T = 0.5$ , and  $L_t$  is varied to vary  $\zeta$ .

tion in (23) accurately anticipates the error in the propagation delay due to neglecting inductance and can be treated as a useful metric to determine when inductance should be included in an interconnect model. Note also that the error is less than 1% for  $\zeta > 1.5$ , permitting the  $RC$  model to be applicable with minimal error for  $\zeta > 1.5$ . However, for small  $\zeta$  ( $\zeta < 1$ ), the error rapidly increases (the error is 30% for  $\zeta = 0.5$ ). Inductance should be included within the interconnect model to maintain sufficient accuracy for small  $\zeta$ . Low-resistance wide wires (and thus low  $\zeta$ ) are frequently encountered in clock distribution networks and certain critical global interconnect (such as data busses). More accurate  $RLC$  models are required for these global interconnect lines particularly since accuracy is of great importance for these nets. Typical values of line parameters for  $0.25\text{-}\mu\text{m}$  CMOS technology are given in Appendix A for different line widths and lengths. Note that lines of widths  $2.4$  and  $7.5 \mu\text{m}$  have a value of  $\zeta$  significantly less than  $1.5$  for almost all wire lengths. These dimensions are common widths of global wires which can therefore exhibit significant inductance effects. This characteristic demonstrates that large errors can be encountered in current VLSI circuits if inductance is neglected. AS/X simulations of CMOS gates driving copper interconnect lines from a  $0.25\text{-}\mu\text{m}$  CMOS technology are shown in Fig. 5. The simulations in Fig. 5 compare the two cases of modeling an interconnect line as an  $RLC$  transmission line and as an  $RC$  transmission line for several driver widths and line dimensions. The error in the propagation delay due to neglecting inductance can be as high as 58% for wide drivers and wide wires. What makes these errors even more serious is that neglecting inductance and using an  $RC$  model rather than an  $RLC$  model always results in underestimating the propagation delay. Thus, VLSI circuits designed using an  $RC$  interconnect model may not satisfy the assigned performance targets despite a worst case analysis being applied in the circuit design process while maintaining safety factors.

### C. Dependence of Delay on Interconnect Length

An interesting special case occurs when the gate parasitic impedances ( $C_L$  and  $R_{tr}$ ) are neglected. This case is particularly

important since it describes the propagation delay characteristics of a distributed  $RLC$  line without the distortion of the gate impedances. In this case, the propagation delay in (18) can be expressed as

$$t_{pd} = \sqrt{LC}(e^{2.9(\alpha_{\text{asym}}l)^{1.35}}l + 0.74\alpha_{\text{asym}}l^2) \quad (24)$$

where

$$\alpha_{\text{asym}} = \frac{R}{2} \sqrt{\frac{C}{L}}. \quad (25)$$

$\alpha_{\text{asym}}$  is the asymptotic value at high frequencies of the attenuation per unit length of the signals as the signals propagate across a lossy transmission line. This expression is given in [13] and has the dimensions of nepers/cm [21].

For the limiting case where  $L \rightarrow 0$ , (24) reduces to  $0.37RCl^2$ . This expression is the same formula for the propagation delay of a distributed  $RC$  line as described in [1], [5], and [16]. Also note the well-known square dependence on the length of the wire. For the other limiting case where  $R \rightarrow 0$ , the propagation delay is given by  $l\sqrt{LC}$ . Note the linear dependence on the length of the line. The solution for the limiting case where  $R \rightarrow 0$  is explained by noting that a distributed  $RLC$  line with zero resistance is simply a lossless transmission line. For a lossless transmission line, the speed at which a signal propagates is

$$v = \frac{1}{\sqrt{LC}}. \quad (26)$$

The time of flight of the signals across a lossless transmission line is  $l/v = l\sqrt{LC}$  [21]. Thus, for a lossless transmission line, the propagation delay (in the case of  $R_{tr} = 0$ ) is  $l\sqrt{LC}$ , which is the physically-based minimum limit for the propagation delay of an  $RLC$  line. This agreement between the general delay model in (18) and an  $LC$  transmission line demonstrates that the limiting case of an  $LC$  line can also be accurately described by (18).

The traditional quadratic dependence of the propagation delay on the length of an  $RC$  line approaches a linear dependence as inductance becomes more significant. According to (24), the parameter that describes this dependence on the interconnect length is  $\alpha_{\text{asym}}$ . As described in [8], [10], and [23], signals propagate across a transmission line in two primary modes. The first mode is the propagation mode in which the signals travel at a constant velocity across the line and the delay is linear with the length of the interconnect. The second mode is the diffusion mode in which the signals diffuse through the line and the propagation delay is quadratic with the length of the interconnect. When there is no attenuation ( $\alpha_{\text{asym}} = 0$ ), the signals propagate purely in the propagation mode as in the case of a lossless transmission line, and, therefore,  $t_{pd} \propto l$ . When the attenuation is large ( $\alpha_{\text{asym}} > 1$ ), the signals propagate primarily in the diffusion mode as in the case of an  $RC$  transmission line and therefore,  $t_{pd} \propto l^2$ . Thus,  $\alpha_{\text{asym}}$  describes the dependence of the propagation delay on the interconnect length. This

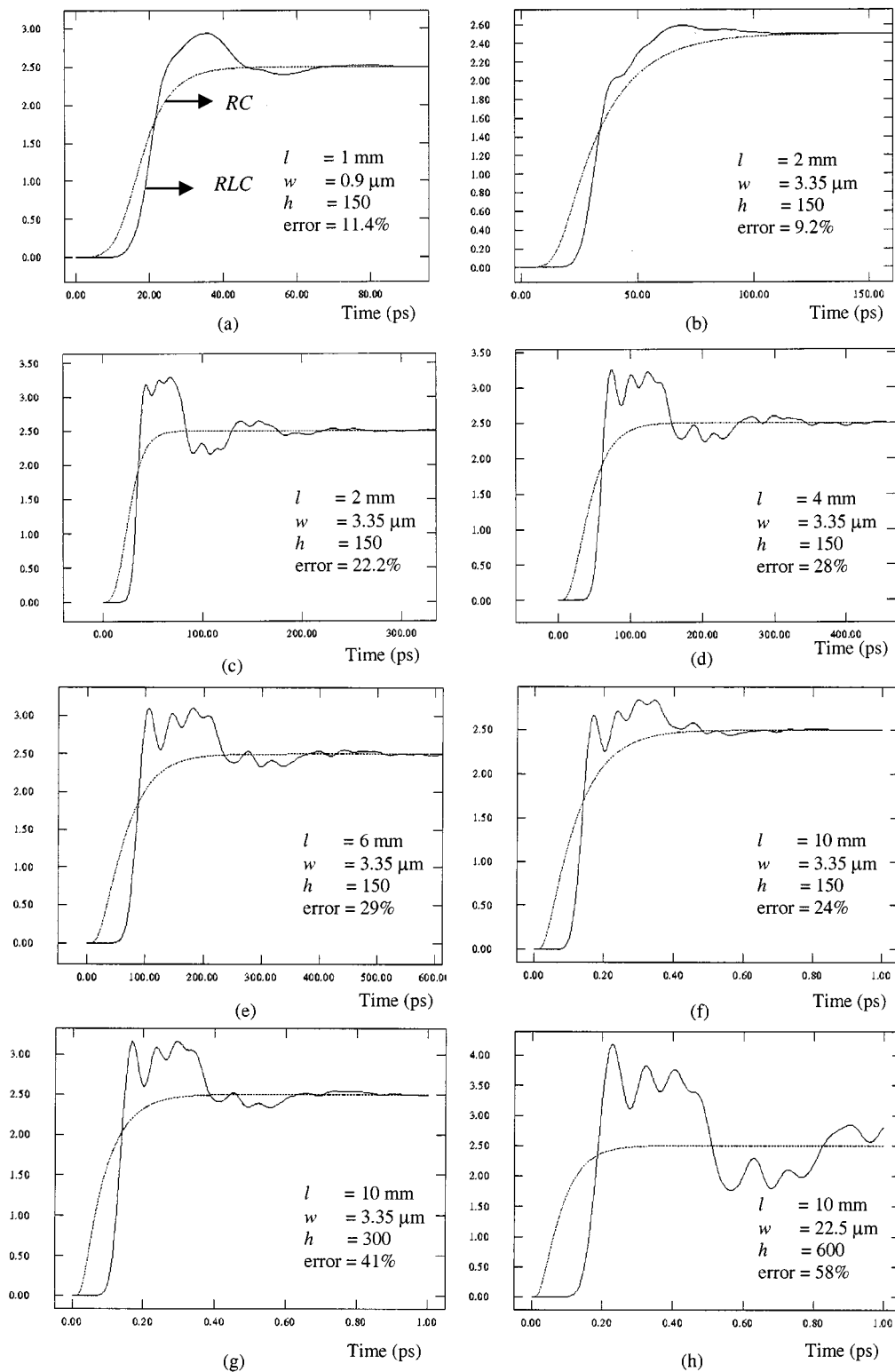


Fig. 5. AS/X simulations of a CMOS gate driving a copper interconnect line based on 0.25- $\mu\text{m}$  CMOS technology. The lines are modeled as  $RC$  lines and as  $RLC$  lines, and the two models are compared to characterize the effects of neglecting inductance. The wire length  $l$ , width  $w$ , and the size of the driving CMOS inverter as compared to a minimum size inverter  $h$  are shown in Fig. 5(a)–(h). The percent error at the 50% delay point between the two models is also shown.

behavior is illustrated in Fig. 6. Note that for  $\alpha_{\text{asym}} > 1$ , the dependence on  $l$  is quadratic for all practical purposes. For  $\alpha_{\text{asym}} < 1$ , the square dependence is far from accu-

rate which can have a profound effect on determining an optimum strategy for driving an interconnect line such as repeater insertion [14]–[17] and transistor sizing [18], [19].

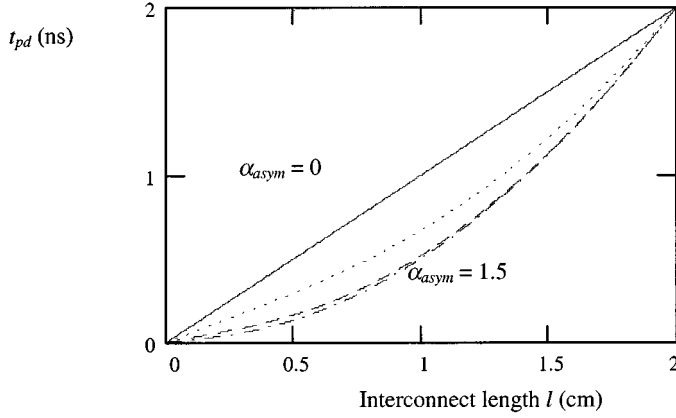


Fig. 6. Dependence of the propagation delay on the length of the interconnect  $l$  ignoring the effects of the gate impedances. The curves represent  $\alpha_{\text{asym}} = 0, 0.5, 1.0, \text{ and } 1.5$  starting from the top curve.

### III. REPEATER INSERTION FOR AN $RLC$ INTERCONNECT

Traditionally, repeaters are inserted into  $RC$  lines to partition an interconnect line into shorter sections [14]–[19], thereby reducing the total propagation delay. Applying the same idea to the general case of an  $RLC$  line, repeaters are used to divide the interconnect line into  $k$  sections as shown in Fig. 7. The buffers are each uniformly the same size and  $h$  times larger than a minimum size buffer. The buffer output impedance  $R_{tr}$  is  $R_0/h$  and the input capacitance of the buffer  $C_L$  is  $hC_0$ . The total propagation delay of the repeater system is the sum of the individual propagation delays of the  $k$  sections and is a function of  $h$  and  $k$  for a given interconnect line. The values of  $h$  and  $k$  at which the total delay  $t_{\text{pdtotal}}$  is a minimum is determined by simultaneously solving the following two differential equations:

$$\frac{\partial t_{\text{pdtotal}}(h, k)}{\partial h} = 0 \quad (27)$$

$$\frac{\partial t_{\text{pdtotal}}(h, k)}{\partial k} = 0. \quad (28)$$

For the special case of an  $RC$  line ( $L_t \rightarrow 0$ ), the solution for these equations is

$$h_{\text{opt}}(RC) = \sqrt{\frac{R_0 C_t}{R_t C_0}} \quad (29)$$

$$k_{\text{opt}}(RC) = \sqrt{\frac{R_t C_t}{2R_0 C_0}}. \quad (30)$$

These equations are the same as described by Bakoglu in [16].

Solving (27) and (28) for the general case of an  $RLC$  line is analytically intractable. However, as described in Appendix B,  $h_{\text{opt}}$  and  $k_{\text{opt}}$  for an  $RLC$  line have the form

$$h_{\text{opt}} = \sqrt{\frac{R_0 C_t}{R_t C_0}} \cdot h'(T_{L/R}) \quad (31)$$

$$k_{\text{opt}} = \sqrt{\frac{R_t C_t}{2R_0 C_0}} \cdot k'(T_{L/R}) \quad (32)$$

where  $h'(T_{L/R})$  and  $k'(T_{L/R})$  are error factors that account for the effect of the inductance and  $T_{L/R}$  is

$$T_{L/R} = \sqrt{\frac{L_t / R_t}{R_0 C_0}}. \quad (33)$$

The closed-form solution for the propagation delay in (18) is used to characterize the delay of the repeater system shown in Fig. 7 as described in Appendix B [see (42)–(46)]. The resulting expression is partially differentiated with respect to  $h$  and  $k$  and the two derivatives are equated to zero. The resulting two equations are solved numerically for the optimum values of  $h$  and  $k$  ( $h_{\text{opt}}$  and  $k_{\text{opt}}$ ). The values of  $h'(T_{L/R})$  and  $k'(T_{L/R})$  are found using (31) and (32) as

$$h'(T_{L/R}) = \frac{h_{\text{opt}}}{\sqrt{\frac{R_0 C_t}{R_t C_0}}} \quad (34)$$

$$k'(T_{L/R}) = \frac{k_{\text{opt}}}{\sqrt{\frac{R_t C_t}{2R_0 C_0}}}. \quad (35)$$

$h'$  and  $k'$  as functions of  $T_{L/R}$  are plotted in Fig. 8. The interconnect and device technology parameters used to generate Fig. 8 are  $R_t = 100 \Omega$ ,  $C_t = 1 \text{ pF}$ ,  $R_0 = 1500 \Omega$ , and  $C_0 = 2 \text{ fF}$ , and  $L_t$  is varied to vary  $T_{L/R}$ . Once  $h'$  and  $k'$  are characterized as functions of  $T_{L/R}$  based on any interconnect and technology parameters,  $h'$  and  $k'$  can be used in (31) and (32) with any other interconnect and technology parameters ( $R_t$ ,  $C_t$ ,  $L_t$ ,  $R_0$ , and  $C_0$ ). Curve fitting is employed to determine a function that accurately characterizes  $h_{\text{opt}}$  and  $k_{\text{opt}}$ . These functions are

$$h_{\text{opt}} = \sqrt{\frac{R_0 C_t}{R_t C_0}} \frac{1}{[1 + 0.16(T_{L/R})^3]^{0.24}} \quad (36)$$

and

$$k_{\text{opt}} = \sqrt{\frac{R_t C_t}{2R_0 C_0}} \frac{1}{[1 + 0.18(T_{L/R})^3]^{0.3}}. \quad (37)$$

These closed-form solutions are highly accurate with an error in the total propagation delay of the repeater system of less than 0.05% as compared to numerical analysis. These formulas can therefore be considered exact for all practical purposes.

Upon examination of (36) and (37),  $h_{\text{opt}}$  and  $k_{\text{opt}}$  are equal to  $h_{\text{opt}}(RC)$  and  $k_{\text{opt}}(RC)$  in (29) and (30) for the special case of an  $RC$  impedance where  $L_t \rightarrow 0$  (or  $T_{L/R} \rightarrow 0$ ). A plot of  $k_{\text{opt}}$  based on both an  $RC$  model and an  $RLC$  model versus  $T_{L/R}$  is shown in Fig. 9. Note that the error between the two cases increases as  $T_{L/R}$  increases. This behavior is understandable since inductance effects are more significant as  $T_{L/R}$  increases (which increases the error of neglecting  $L_t$ ). Also note that as  $T_{L/R}$  increases (or the inductance effects increase), the number of sections  $k_{\text{opt}}$  decreases. This behavior is intuitively understandable by referring to the results of Fig. 6 and noting that  $T_{L/R}$  can be expressed as

$$T_{L/R} = \frac{1}{2\alpha_{\text{asym}}} \sqrt{\frac{RC}{R_0 C_0}}. \quad (38)$$

Note that as  $\alpha_{\text{asym}}$  decreases,  $T_{L/R}$  increases. As shown in Fig. 6, the dependence of the propagation delay of an  $RLC$  line on the length of the interconnect is linear when  $\alpha_{\text{asym}} = 0$  (i.e., very high inductive effects) and quadratic when  $\alpha_{\text{asym}} \rightarrow \infty$  (i.e., no inductive effects). In general, the dependence of the propagation delay of an  $RLC$  line on the length of the interconnect is bounded between a linear and quadratic relationship

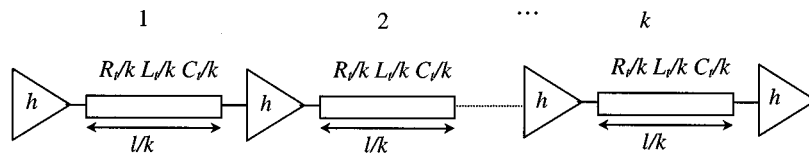


Fig. 7. Repeaters inserted in an  $RLC$  line to minimize the propagation delay.

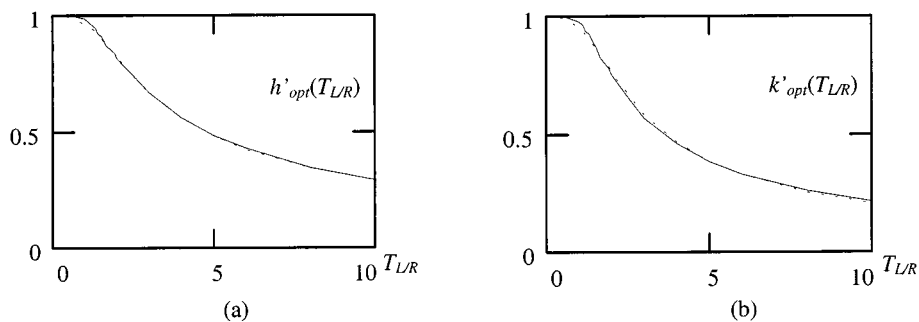


Fig. 8. Numerical solutions of (27) and (28) and (36) and (37) for (a)  $h_{opt}$  and (b)  $k_{opt}$ , respectively. Numerical solutions are shown by the solid line while (36) and (37) are shown by the dashed line.

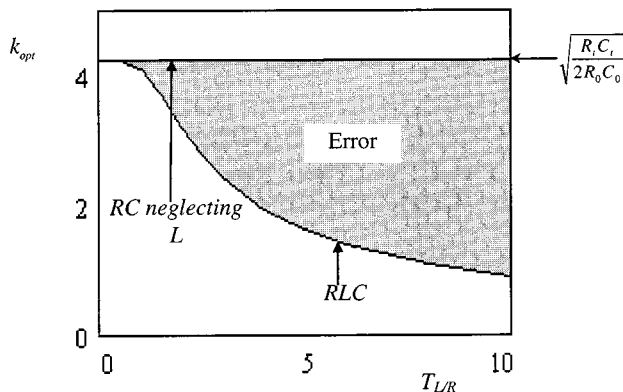


Fig. 9. The number of sections  $k_{opt}$  that minimizes the propagation delay of an  $RLC$  line as a function of  $T_{L/R}$ . The cases where the inductance is neglected and where the inductance is included are considered. Note that the error between the two cases increases as  $T_{L/R}$  increases.

depending on the value of  $\alpha_{asym}$ . The improvement achieved by partitioning the line into shorter sections in the  $RC$  case is primarily due to this quadratic dependence of the propagation delay on  $l$ . In the other extreme case where  $\alpha_{asym} = 0$ , the propagation delay is linear with  $l$  and therefore no speed improvement is achieved by dividing the line into shorter sections. Actually, adding repeaters in this case would only increase the total propagation delay because of the additional gate delay of the repeaters. Thus, as inductance effects increase, the optimum number of repeaters inserted to minimize the total interconnect delay decreases.

The percent increase in  $t_{pdtotal}$  caused by neglecting inductance and treating an  $RLC$  line as an  $RC$  line as compared to

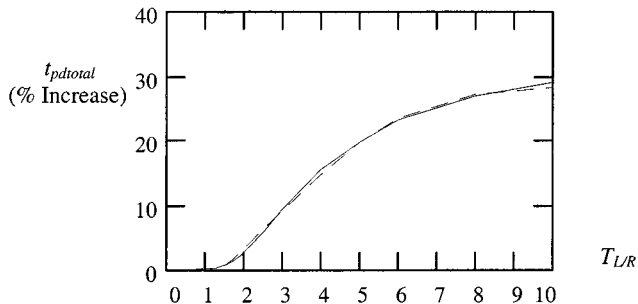


Fig. 10. The increase in  $t_{pdtotal}$  if inductance is neglected as a function of  $T_{L/R}$ . Numerical solutions are designated by the solid line while (40) is designated by the dashed line.

including inductance based on (36) and (37) for  $h_{opt}$  and  $k_{opt}$ , respectively, is

$$\% \text{Increase} = \frac{100 \cdot [(t_{pdtotal})_{RC} - (t_{pdtotal})_{RLC}]}{(t_{pdtotal})_{RLC}}, \quad (39)$$

$(t_{pdtotal})_{RC}$  is calculated by substituting the solution for  $h_{opt}(RC)$  and  $k_{opt}(RC)$  in (29) and (30) into  $t_{pdtotal}$ .  $(t_{pdtotal})_{RLC}$  is calculated by substituting the solution for  $h_{opt}$  and  $k_{opt}$  in (36) and (37), respectively, into  $t_{pdtotal}$ . The resulting solution is a function of  $T_{L/R}$  only and can be accurately approximated by

$$\% \text{Increase} = \frac{30}{\sqrt{\left(1 + \frac{0.5}{T_{L/R}} + 23e^{0.8T_{L/R}} + 10^4 e^{-4T_{L/R}}\right)}}. \quad (40)$$

The percent increase in  $t_{\text{pdtotal}}$  over the  $RLC$  case is plotted in Fig. 10. Note that  $(t_{\text{pdtotal}})_{RC}$  is larger compared to  $(t_{\text{pdtotal}})_{RLC}$  as  $T_{L/R}$  increases. For  $T_{L/R} = 3$ ,  $t_{\text{pdtotal}}$  increases by 10%. For  $T_{L/R} = 5$ ,  $t_{\text{pdtotal}}$  increases by 20%. For  $T_{L/R} = 10$ ,  $t_{\text{pdtotal}}$  increases by 30%.

The total area of the buffers in the repeater system is given by  $A_{RLC} = h_{\text{opt}} \cdot k_{\text{opt}} \cdot A_{\text{min}}$  and  $A_{RC} = h_{\text{opt}}(RC) \cdot k_{\text{opt}}(RC) \cdot A_{\text{min}}$  for the  $RLC$  and the  $RC$  case, respectively.  $A_{\text{min}}$  is the area of a minimum size buffer. The percent area increase  $\%AI$  is characterized by  $100 \cdot (A_{RC} - A_{RLC})/A_{RLC}$  and is

$$\%AI = 100\{[1 + 0.18(T_{L/R})^3]^{0.3} \cdot [1 + 0.16(T_{L/R})^3]^{0.24} - 1\}. \quad (41)$$

The percent area increase for  $T_{L/R} = 3$  is 154% and for  $T_{L/R} = 5$  is 435%. Thus, neglecting inductance not only increases the total delay of the repeater system, but significantly increases the buffer area as well. This trend is expected since treating the interconnect as an  $RC$  line and neglecting inductance requires more repeaters. These extra repeaters add to the total delay and buffer area without reducing the line delay because inductance makes the dependence of the delay on the length of the interconnect subquadratic. Although the effect of inductance on the power dissipated by the repeater system has not been quantitatively characterized in this paper, it is expected that considering inductance in the interconnect model would result in a repeater system that consumes less power due to the decreased buffer capacitance and width.

As described in Appendix A,  $T_{L/R} > 3$  is common for a wide range of on-chip interconnect and  $T_{L/R}$  approaches ten for wider interconnects commonly seen in a typical  $0.25\text{-}\mu\text{m}$  CMOS technology. Thus, the propagation delay of a repeater system can increase in a standard  $0.25\text{-}\mu\text{m}$  CMOS technology by up to 30% and the buffer area by up to 15 times if inductance is neglected. Note also that  $T_{L/R}$  increases as  $R_0C_0$  decreases. This relation means that as the gate delay decreases, inductance becomes more important. Thus, the effects of inductance in next generation design methodologies will become fundamentally important as technologies scale.

This trend can be explained intuitively by examining the special case of a line with large inductance effects. As discussed before, the minimum total propagation delay can be achieved for such a line by not inserting any buffers independent of the intrinsic speed of the technology. If inductance is ignored and an  $RC$  model is used for such a line, the number of buffers that are inserted will increase as the buffers become faster since there is less of a penalty for inserting more buffers. Thus, the discrepancy between the buffer solutions based on an  $RC$  and an  $RLC$  model (zero buffer area for dominant inductance effects) increases as faster buffers are used. In general, the buffer area required to minimize the total propagation delay based on an  $RC$  model increases more rapidly when the devices become faster as compared to an  $RLC$  model.

Finally, in estimating the effects of inductance on the repeater insertion process, an equivalent linear resistor is used to model the nonlinear CMOS transistors. This linearization

TABLE II  
INTERCONNECT PARAMETERS FOR DIFFERENT LINE WIDTHS [12]

Width ( $\mu\text{m}$ )	$R$ ( $\Omega/\text{cm}$ )	$L$ (nH/cm)	$C$ (pF/cm)
0.9	494	4.75	1.73
1.8	248	3.70	1.85
2.4	76	5.30	2.60
7.5	35	3.47	5.16

of the transistors results in an overestimation of inductance effects. This behavior can be understood by noting that a transistor in a CMOS gate operates partially in the linear region and partially in the saturation region during switching. In the linear region, the transistor can be accurately approximated by a resistor. However, in the saturation region, the transistor is more accurately modeled as a current source with a parallel high resistance. The Thevenin equivalent of this circuit is a voltage source with a high resistance in series. This high resistance in series with an interconnect line overrides the series resistance and inductance of the line. Thus, the interconnect appears predominantly capacitive when the transistor operates in the saturation region and the effect of inductance (and resistance) is negligible. If the transistor operates in the saturation region during the entire switching time, there is very small error due to neglecting inductance (and resistance). Since the transistor operates partially in the linear region and partially in the saturation region, the metrics presented in this paper represent worst case inductance effects.

#### IV. CONCLUSIONS

Closed-form solutions for the propagation delay of a CMOS gate driving a distributed  $RLC$  load are presented that are within 5% of AS/X simulations. It is shown that neglecting inductance can cause large errors (over 35%) in the propagation delay for current on-chip interconnect. It is also shown that the traditional quadratic dependence of the propagation delay on the length of the interconnect for  $RC$  lines tends to a linear dependence as inductance effects increase. This behavior is expected to have a profound effect on future high-speed CMOS technologies.

Closed-form solutions are presented for inserting repeaters into  $RLC$  lines that are highly accurate with respect to numerical solutions. The process of inserting repeaters into  $RLC$  lines increases the propagation delay by up to 30% if inductance is neglected as compared to applying a distributed  $RLC$  impedance model of the interconnect. Thus, incorporating inductance into the impedance model of the interconnect is of crucial importance for estimating and minimizing the propagation delay of on-chip interconnect. This importance is expected to increase as the gate parasitic impedances decrease and as technologies increase in speed. Future work includes using more accurate gate models, determining delay formulas for  $RLC$  trees and characterizing the effects of inductance on the repeater insertion process in tree structured on-chip interconnect.

TABLE III  
 $\zeta$  AND  $T_{L/R}$  FOR DIFFERENT LINE WIDTHS AND LENGTHS IN A CURRENT 0.25- $\mu\text{m}$  CMOS TECHNOLOGY

Line width ( $\mu\text{m}$ )	Buffer width $h$	$\zeta$					$T_{L/R}$
		Line length (mm)					
		2	4	6	8	10	
0.9	40	1.327	1.770	2.235	2.702	3.171	1.096
	80	1.299	1.790	2.272	2.750	3.226	
	120	1.397	1.930	2.443	2.930	3.422	
	240	1.743	2.426	3.015	3.562	4.087	
1.8	40	1.101	1.337	1.600	1.870	2.143	1.366
	80	0.936	1.200	1.473	1.749	2.026	
	120	0.940	1.233	1.519	1.803	2.085	
	240	1.082	1.456	1.79	2.104	2.407	
2.4	40	0.752	0.800	0.871	0.949	1.029	2.952
	80	0.498	0.554	0.628	0.707	0.788	
	120	0.429	0.491	0.568	0.648	0.732	
	240	0.390	0.473	0.560	0.647	0.733	
7.5	40	1.118	1.151	1.206	1.268	1.332	3.525
	80	0.647	0.683	0.739	0.801	0.865	
	120	0.497	0.535	0.592	0.654	0.719	
	240	0.362	0.410	0.470	0.535	0.600	

APPENDIX A  
INDUSTRIAL VALUES FOR  $\zeta$  AND  $T_{L/R}$

For a current 0.25- $\mu\text{m}$  CMOS technology, experimentally measured interconnect parameters ( $R$ ,  $L$ , and  $C$ ) are provided in [12] for different line widths and are listed here in Table II. These line parameters are used in this paper to evaluate  $\zeta$  and  $T_{L/R}$  for different line geometries as shown in Table III. The data listed in Table III also include the effects of the driver output impedance and the load capacitance on  $\zeta$  and  $T_{L/R}$ .  $h$  represents the size of the driver and the load gates (assumed to be of equal size) and is with respect to a minimum size buffer. Thus,  $R_{tr} = R_0/h$  and  $C_L = hC_0$ . Note that  $T_{L/R}$  is independent of the length of the wire. Note also that the values of  $\zeta$  are significantly less than one for common width wires which implies that significant errors in the propagation delay will be incurred. The values indicated for  $T_{L/R}$  demonstrate that large errors can be encountered in the repeater insertion process if an  $RC$  model rather than an  $RLC$  model is used.

APPENDIX B  
OPTIMUM REPEATER INSERTION IN  $RLC$  LINES

As shown in Section II, the propagation delay of a CMOS gate driving a single section of interconnect with parameters of  $R_t$ ,  $C_t$ , and  $L_t$  has the form given by (16). If repeaters are inserted to divide the line into  $k$  sections and each repeater is  $h$  times greater than a minimum size inverter, the total propagation delay of the system is the summation of the propagation delays of each of the sections. Since the delay of each section is equal, the total delay can be expressed as  $t_{pd\text{total}} = k t_{pds}$ , where  $t_{pds}$  is the propagation delay of a single section. Each section has interconnect parameters equal to  $R_t/k$ ,  $C_t/k$ , and  $L_t/k$ . Since each repeater is  $h$  times larger than a minimum size buffer, each repeater has an output resistance  $R_{tr} = R_0/h$  and a

load capacitance  $C_L = C_0 h$ . Thus, the total propagation delay of the repeater system is

$$t_{pd\text{total}} = k \cdot \frac{t'_{pd}(\zeta_{\text{sec}}, R_{T\text{sec}}, C_{T\text{sec}})}{\omega_{n\text{sec}}} \quad (42)$$

where  $R_{T_s}$  and  $C_{T_s}$  are

$$R_{T\text{sec}} = \frac{k}{h} \frac{R_0}{R_t} \quad (43)$$

$$C_{T\text{sec}} = kh \frac{C_0}{C_t} \quad (44)$$

$\zeta_s$  and  $\omega_{ns}$  are

$$\zeta_{\text{sec}} = \frac{R_t}{2k} \sqrt{\frac{C_t}{L_t}} \cdot \frac{R_{T\text{sec}} + C_{T\text{sec}} + R_{T\text{sec}} C_{T\text{sec}} + 0.5}{\sqrt{(1 + C_{T\text{sec}})}} \quad (45)$$

$$\omega_{n\text{sec}} = \frac{k}{\sqrt{L_t C_t} \sqrt{1 + C_{T\text{sec}}}} \quad (46)$$

The solution for the general case of an  $RLC$  interconnect is in the form of

$$h = \sqrt{\frac{R_0 C_t}{T_t C_0}} \cdot h' \quad (47)$$

$$k = \sqrt{\frac{R_t C_t}{2R_0 C_0}} \cdot k' \quad (48)$$

where  $h'$  and  $k'$  are error factors due to the existence of inductance and approach one as the inductance approaches zero. Substituting these values for  $h$  and  $k$  into (43)–(46), the variables  $R_{T_s}$ ,  $C_{T_s}$ ,  $\zeta_s$ , and  $\omega_{ns}$  are

$$R_{T\text{sec}} = \frac{k'}{h' \sqrt{2}} \quad (49)$$

$$C_{T\text{sec}} = \frac{h' k'}{\sqrt{2}} \quad (50)$$

$$\zeta_{\text{sec}} = \frac{1}{\sqrt{2} k' T_{L/R}} \cdot \frac{R_{T\text{sec}} + C_{T\text{sec}} + R_{T\text{sec}} C_{T\text{sec}} + 0.5}{\sqrt{(1 + C_{T\text{sec}})}} \quad (51)$$

and

$$\frac{k}{\omega_{nsec}} = \sqrt{L_t C_t} \sqrt{(1 + C_{Tsec})} \quad (52)$$

where  $T_{L/R}$  is given by

$$T_{L/R} = \sqrt{\frac{L_t/R_t}{R_0 C_0}}. \quad (53)$$

Substituting (49)–(52) in (42), the total propagation delay has the form

$$t_{pdtotal} = \sqrt{L_t C_t} \cdot f(h', k', T_{L/R}). \quad (54)$$

Determining the values of  $k'$  and  $h'$  that minimize the total propagation delay requires the simultaneous solution of the following two differential equations:

$$\frac{\partial f(h', k', T_{L/R})}{\partial h'} = 0 \quad (55)$$

$$\frac{\partial f(h', k', T_{L/R})}{\partial k'} = 0. \quad (56)$$

Thus, the optimum number of sections  $k_{opt}$  and the optimum repeater size  $h_{opt}$  to minimize the propagation delay of an *RLC* interconnect are only functions of  $T_{L/R}$  and are

$$h_{opt} = \sqrt{\frac{R_0 C_t}{R_t C_0}} \cdot h'(T_{L/R}) \quad (57)$$

$$k_{opt} = \sqrt{\frac{R_t C_t}{2R_0 C_0}} \cdot k'(T_{L/R}). \quad (58)$$

Note that this solution is characteristic of an *RLC* line and that no approximations have been made in deriving this result.

## REFERENCES

- [1] J. M. Rabaey, *Digital Integrated Circuits, A Design Perspective*. Englewood Cliffs, NJ: Prentice-Hall, 1996.
- [2] D. A. Priore, "Inductance on silicon for sub-micron CMOS VLSI," in *Proc. IEEE Symp. VLSI Circuits*, May 1993, pp. 17–18.
- [3] D. B. Jarvis, "The effects of interconnections on high-speed logic circuits," *IEEE Trans. Electron. Computers*, vol. EC-10, pp. 476–487, Oct. 1963.
- [4] M. P. May, A. Taflove, and J. Baron, "FD-TD modeling of digital signal propagation in 3-D circuits with passive and active loads," *IEEE Trans. Microwave Theory Tech.*, vol. 42, pp. 1514–1523, Aug. 1994.
- [5] T. Sakurai, "Approximation of wiring delay in MOSFET LSI," *IEEE J. Solid-State Circuits*, vol. SC-18, pp. 418–426, Aug. 1983.
- [6] G. Y. Yacoub, H. Pham, and E. G. Friedman, "A system for critical path analysis based on back annotation and distributed interconnect impedance models," *Microelectron J.*, vol. 18, no. 3, pp. 21–30, June 1988.
- [7] Y. Eo and W. R. Eisenstadt, "High-speed VLSI interconnect modeling based on S-parameter measurement," *IEEE Trans. Comp., Hybrids, Manufact. Technol.*, vol. 16, pp. 555–562, Aug. 1993.
- [8] M. Shoji, *High-Speed Digital Circuits*. Reading, MA: Addison-Wesley, 1996.
- [9] J. Torres, "Advanced copper interconnections for silicon CMOS technologies," *Applied Surface Sci.*, vol. 91, no. 1, pp. 112–123, Oct. 1995.
- [10] A. Deutsch *et al.*, "High-speed signal propagation on lossy transmission lines," *IBM J. Res. Develop.*, vol. 34, no. 4, pp. 601–615, July 1990.
- [11] —, "Modeling and characterization of long interconnections for high-performance microprocessors," *IBM J. Res. Develop.*, vol. 39, no. 5, pp. 547–667, Sept. 1995.
- [12] —, "When are transmission-line effects important for on-chip interconnections?," *IEEE Trans. Microwave Theory Tech.*, vol. 45, pp. 1836–1846, Oct. 1997.
- [13] Y. I. Ismail, E. G. Friedman, and J. L. Neves, "Figures of merit to characterize the importance of on-chip inductance," in *Proc. IEEE/ACM Design Automation Conf.*, June 1998, pp. 560–565.
- [14] H. B. Bakoglu and J. D. Meindl, "Optimal interconnection circuits for VLSI," *IEEE Trans. Electron Devices*, vol. ED-32, pp. 903–909, May 1985.
- [15] L. P. Ginneken, "Buffer placement in distributed RC-tree networks for minimal Elmore delay," in *Proc. IEEE Int. Symp. Circuits Syst.*, May 1990, pp. 865–868.
- [16] H. B. Bakoglu, *Circuits, Interconnections, and Packaging for VLSI*. Reading, MA: Addison-Wesley, 1990.
- [17] V. Adler and E. G. Friedman, "Repeater design to reduce delay and power in resistive interconnect," *IEEE Trans. Circuits Syst. II*, vol. 45, pp. 607–616, May 1998.
- [18] S. Dhar and M. A. Franklin, "Optimum buffer circuits for driving long uniform lines," *IEEE J. Solid-State Circuits*, vol. 26, pp. 32–40, Jan. 1991.
- [19] C. J. Alpert, "Wire segmenting for improved buffer insertion," in *Proc. IEEE/ACM Design Automation Conf.*, June 1997, pp. 588–593.
- [20] *AS/X User's Guide*, IBM Corp., NY, 1996.
- [21] L. N. Dworsky, *Modern Transmission Line Theory and Applications*. New York: Wiley, 1979.
- [22] W. C. Elmore, "The transient response of damped linear networks," *J. Appl. Physics*, vol. 19, pp. 55–63, Jan. 1948.
- [23] E. Weber, *Linear Transient Analysis*. New York: Wiley, 1956, vol. II.



**Yehya I. Ismail** received the B.S. degree in electronics and communications engineering (with honors) from Cairo University, Cairo, Egypt, in 1993, the Master's degree in electronics from Cairo University (with distinction) in 1996, and the Master's degree in electrical engineering from the University of Rochester, Rochester, NY, in 1998. He is currently working toward the Ph.D. degree in the area of high-performance VLSI IC design at the University of Rochester.

He was with the IBM Cairo Scientific Center (CSC) from 1993 to 1996 and IBM Microelectronics, East Fishkill, NY, during the summers of 1997–1999. His primary research interests include interconnect, noise, and related circuit level issues in high-performance VLSI circuits.



**Eby G. Friedman** (S'78–M'79–SM'90–F'00) received the B.S. degree from Lafayette College, Easton, PA, in 1979 and the M.S. and Ph.D. degrees from the University of California, Irvine, in 1981 and 1989, respectively, all in electrical engineering.

From 1979 to 1991, he was with Hughes Aircraft Company, where he was Manager of the Signal Processing Design and Test Department responsible for the design and test of high-performance digital and analog IC's. He has been with the Department of Electrical and Computer Engineering, University of Rochester, Rochester, NY, since 1991, where he is a Professor and the Director of the High Performance VLSI/IC Design and Analysis Laboratory and Director of the Center for Electronic Imaging Systems. His current research and teaching interests are in high-performance synchronous digital and mixed-signal microelectronic design and analysis with application to high-speed portable processors and low-power wireless communications. He is the author of more than 135 papers and book chapters and the author or editor of four books in the fields of high-speed and low-power CMOS design techniques, high-speed interconnect, and the theory and application of synchronous clock distribution networks. He is a Member of the Editorial Board of the IEEE TRANSACTIONS ON CIRCUITS AND SYSTEMS II: ANALOG AND DIGITAL SIGNAL PROCESSING.

Dr. Friedman is a Regional Editor of the *Journal of Circuits, Systems, and Computers*, a Member of the Editorial Board of *Analog Integrated Circuits and Signal Processing* and the CAS BoG, Chair of the IEEE TRANSACTIONS ON VERY LARGE SCALE INTEGRATION (VLSI) SYSTEMS Steering Committee, and a Member of the Technical Program Committee of a number of conferences. He previously was a Chair of the VLSI Systems and Applications CAS Technical Committee, the Electron Devices Chapter of the IEEE Rochester Section, and the VLSI track for ISCAS '96 and '97. He was Technical Cochair of the 1997 IEEE International Workshop on Clock Distribution Networks and the Editor of several special issues in a variety of journals. He is the recipient of the Howard Hughes Masters and Doctoral Fellowships, an IBM University Research Award, an Outstanding IEEE Chapter Chairman Award, and a University of Rochester College of Engineering Teaching Excellence Award.